



**Providing Choice & Value**  
Generic CT and MRI Contrast Agents

**FRESENIUS  
KABI**

**CONTACT REP**

**AJNR**

## **MRI for Cushing Disease: A Systematic Review**

M. Castle-Kirszbaum, S. Amukotuwa, P. Fuller, T. Goldschlager, A. Gonzalvo, J. Kam, C.Y. Kow, M.D. Shi and S. Stuckey

This information is current as of July 29, 2025.

*AJNR Am J Neuroradiol* published online 9 February 2023  
<http://www.ajnr.org/content/early/2023/02/09/ajnr.A7789>

## MRI for Cushing Disease: A Systematic Review

 M. Castle-Kirsbaum,  S. Amukotuwa, P. Fuller,  T. Goldschlager, A. Gonzalvo, J. Kam,  C.Y. Kow,  M.D. Shi, and  S. Stuckey



## ABSTRACT

**BACKGROUND:** MR imaging is key in the diagnostic work-up of Cushing disease. The sensitivity of MR imaging in Cushing disease is not known nor is the prognostic significance of “MR imaging–negative” disease.

**PURPOSE:** Our aim was to determine the overall sensitivity and prognostic significance of MR imaging localization of Cushing disease.

**DATA SOURCES:** We performed a systematic review of the MEDLINE and PubMed databases for cohort studies reporting the sensitivity of MR imaging for the detection of adenomas in Cushing disease.

**STUDY SELECTION:** This study included 57 studies, comprising 5651 patients.

**DATA ANALYSIS:** Risk of bias was assessed using the methodological index for non-randomized studies criteria. Meta-analysis of proportions and pooled subgroup analysis were performed.

**DATA SYNTHESIS:** Overall sensitivity was 73.4% (95% CI, 68.8%–77.7%), and the sensitivity for microadenomas was 70.6% (66.2%–74.6%). There was a trend toward greater sensitivity in more recent studies and with the use of higher-field-strength scanners. Thinner-section acquisitions and gadolinium-enhanced imaging, particularly dynamic sequences, also increased the sensitivity. The use of FLAIR and newer 3D spoiled gradient-echo and FSE sequences, such as spoiled gradient-echo sequences and sampling perfection with application-optimized contrasts by using different flip angle evolutions, may further increase the sensitivity but appear complementary to standard 2D spin-echo sequences. MR imaging detection conferred a 2.63-fold (95% CI, 2.06–3.35-fold) increase in remission for microadenomas compared with MR imaging–negative Cushing disease.

**LIMITATIONS:** Pooled analysis is limited by heterogeneity among studies. We could not account for variation in image interpretation and tumor characteristics.

**CONCLUSIONS:** Detection on MR imaging improves the chances of curative resection of adenomas in Cushing disease. The evolution of MR imaging technology has improved the sensitivity for adenoma detection. Given the prognostic importance of MR imaging localization, further effort should be made to improve MR imaging protocols for Cushing disease.

**ABBREVIATIONS:** ACTH = adrenocorticotrophic hormone; CD = Cushing disease; CRH = corticotropin-releasing hormone; GE = gradient-echo; MINORS = methodological index for non-randomized studies; RARE = rapid acquisition with relaxation excitement; SE = spin-echo; SPGR = spoiled gradient-echo sequences; SPACE = sampling perfection with application-optimized contrasts by using different flip angle evolutions

Cushing disease (CD) is associated with reduced quality of life<sup>1</sup> and excess mortality.<sup>2</sup> MR imaging of the sellar region


identifies most cases of Cushing disease; however, up to 40% of cases are “MR imaging–negative,” though the exact proportion has not been definitively established.<sup>3–5</sup>

Surgeons rely on MR imaging to identify the surgical target, guide surgical planning and technique, and avoid complications. Foremost, adenoma localization facilitates selective adenomec-tomy, which is associated with the highest rate of cure.<sup>6,7</sup> In MR imaging–negative Cushing disease, the surgeon is required to make multiple incisions into the gland in search of adenoma tissue or perform a hemi- or subtotal hypophysectomy;<sup>8</sup> both are associated with a higher rate of complications and a lesser rate of cure.<sup>9,10</sup> Surgical exploration and hemi-hypophysectomy may be

Received February 1, 2022; accepted after revision October 11.

From the Departments of Neurosurgery (M.C.-K., T.G., J.K., C.Y.K.), Radiology (S.A.), Endocrinology (P.F.), and Surgery (M.C.-K., T.G.), Monash Health, Melbourne, Australia; Hudson Institute (P.F.), Melbourne, Australia; Department of Neurosurgery (A.G., J.K.), Austin Hospital, Melbourne, Australia; Barwon Health (M.D.S.), Geelong, Australia; and Department of Radiology (S.S.), Peter MacCallum Cancer Centre, Melbourne, Australia.

Please address correspondence to Mendel Castle-Kirsbaum, MBBS, PhD, Department of Neurosurgery, Monash Health, Melbourne Australia, 246 Clayton Rd, Clayton VIC, Australia 3168; e-mail: mdckjournal@gmail.com

 Indicates article with online supplemental data.

<http://dx.doi.org/10.3174/ajnr.A7789>

guided by inferior petrosal sinus sampling, but this procedure is invasive, not without risk, and correctly lateralizes eccentric tumors in only 69% of cases.<sup>11</sup>

Improved MR imaging detection of adenomas in CD would avoid delays in treatment, streamline surgery, reduce the need for inferior petrosal sinus sampling, minimize iatrogenic gland and stalk injury, obviate the need for hypophysectomy, and increase the chance of surgical cure.<sup>12</sup> We sought to systematically review the literature on MR imaging in CD to establish the rate of MR imaging–negative disease, the patient and imaging protocol factors that determine MR imaging sensitivity, and the association of MR imaging localization with rates of biochemical remission after surgery.

### **Primer of MR Imaging for CD**

MR imaging of the pituitary gland is notoriously challenging due to its anatomy. The pituitary gland sits in the sella at the confluence of the nasal, orbital, and cranial regions,<sup>13,14</sup> medial to the lateral sellar compartment (cavernous sinus, a part of the extradural neuraxial compartment).<sup>15</sup>

A number of artifacts degrade sellar MR imaging. Due to its small size, partial volume effects from adjacent structures such as the ICA, sphenoid sinus air, or cavernous sinus fat may mimic microadenomas. A thin-section, high in-plane resolution, multiplanar acquisition is hence essential.<sup>16</sup> Tissue inhomogeneity is also problematic; changes in magnetic susceptibility at air- and bone–soft tissue interfaces also distort the local magnetic field and cause artifacts, particularly at higher field strengths. Chemical shift artifacts may occur in the setting of fat infiltration of the dorsum sellae or cavernous sinus and may require fat-suppressed imaging. Pulsatile flow in the adjacent ICA,<sup>17</sup> significantly enlarged intercavernous sinuses, or turbulent CSF in the suprasellar cistern may also cause artifacts. Finally, patients with Cushing syndrome may have an empty sella,<sup>18</sup> which may reduce imaging sensitivity through either direct compression or altering the dynamics of contrast within the normal gland.<sup>19</sup>

Standard MR images are pre- and post intravenous gadolinium T1-weighted spin-echo (SE) or rapid acquisition with relaxation enhancement (RARE), eg, FSE/TSE, acquired in the coronal and sagittal planes, and coronal T2-weighted FSE with a section thickness of  $\leq 3$  mm. Volumetric acquisitions are now preferred because these provide thin slices and minimize partial volume effects and have the ability to create multiplanar reformats. Volumetric sequences are usually gradient-echo (GE) or RARE-based. Pituitary adenomas are typically T2-hyperintense and T1-hypointense to the normal gland precontrast; however, they may have a variety of signal characteristics and are often (frustratingly) isointense and imperceptible.

Enhancement is typically delayed compared with the normal gland, with slower wash-in and washout phases.<sup>20</sup> Adenomas, therefore, typically enhance less than the normal pituitary gland in early postcontrast images but display greater enhancement on delayed imaging. The reason is not clear but may relate to poor permeability of the pseudocapsule, reduced vessel density,<sup>21</sup> or a predominance of small vessels within the tumor neovasculature.<sup>22</sup> These enhancement characteristics are exploited by dynamic imaging acquisitions, in which the point of maximal-intensity

difference during wash-in is sought. Multiple (usually 6) sets of coronal T1-weighted images (either 2D or 3D, SE, FSE or GE) are acquired at 10-second intervals immediately following contrast administration. Delayed imaging, 30–60 minutes after contrast administration, may also be performed to take advantage of the relatively slow contrast washout within adenomas. FLAIR imaging is more sensitive to paramagnetic contrast enhancement than T1-weighted images and may, therefore, be preferred in this setting.<sup>23</sup> Spoiled gradient-echo sequences (SPGR) offer greater soft-tissue contrast and allow faster acquisition (minimizing motion/vascular pulsation artifacts) than standard SE sequences.<sup>24</sup> They are also often acquired with thinner slices. However, the SNR may be inferior to that in SE sequences, increasing the rate of false-positive findings, and susceptibility artifacts are also increased. 3D variable flip-angle FSE sequences, such as sampling perfection with application-optimized contrasts by using different flip angle evolutions (SPACE sequence; Siemens), allow thin-section imaging in reasonable acquisition times, reducing partial volume and motion artifacts.<sup>25</sup> These FSE sequences are resistant to susceptibility artifacts compared with 3D GE sequences. They may also be particularly useful for laterally based tumors because the signal intensity of slow-flowing blood (eg, in the cavernous sinus)<sup>26</sup> is high, while flow voids are maintained in fast-flowing carotids.<sup>27</sup> High spatial-resolution balanced spoiled steady-state free precession sequences, such as CISS, are predominantly heavily T2-weighted images that have a high SNR and are relatively insensitive to motion. Acquired without contrast, they may provide complementary findings to standard SE sequences by identifying microcystic or more T2-hyperintense regions in otherwise silent lesions and are suitable for patients with contraindications to intravenous gadolinium.

### **MATERIALS AND METHODS**

A systematic review was performed in accordance with the Preferred Reporting Items for Systematic reviews and Meta-Analyses (PRISMA) statement.<sup>28</sup> A systematic search of the MEDLINE and PubMed electronic databases from their date of inception to September 2021 was conducted using the search string: (Magnetic Resonance Imaging OR MRI OR MR) AND (Cushing(s) Disease OR Corticotroph Adenoma OR Corticotrope Adenoma OR ACTH-Dependent Cushing(s) Syndrome).

Inclusion criteria were defined as the following: 1) randomized and nonrandomized controlled trials and cohort studies that reported the sensitivity of MR imaging for the detection of pituitary adenomas in Cushing disease; 2) documentation of an acceptable “reference standard” diagnosis of Cushing disease (histology or remission after surgery); and 3) written in English. Studies of multiple tumor types in which data specific to CD could not be extracted, studies of imaging modalities in which data specific to MR imaging could not be extracted, and single case reports were excluded.

### **Data Collection**

Data extraction included study year, study size, patient age, surgical status, surgery type, adenoma size, cure rates, and MR imaging protocol. Results were stratified, when possible, by patient age, study year, tumor size, and MR imaging characteristics.

Risk of bias in individual studies was assessed using the methodological index for non-randomized studies (MINORS).<sup>29</sup>

Meta-analysis of proportions was performed using the random-effects model for overall sensitivity. Pooled analysis was performed for subgroup analysis, and the Fisher exact test was used to compare pooled dichotomous data. Statistical significance was defined as  $P < .05$ . Heterogeneity between studies included in the meta-analysis of proportions was measured using the  $I^2$  statistic. Analysis was performed using R 4.1.1 (<http://www.r-project.org/>).

## RESULTS

Fifty-seven studies were identified from the systematic search of the literature (Online Supplemental Data), comprising 5651 patients (Online Supplemental Data). Risk of bias was assessed by the MINORS criteria and is presented in the Online Supplemental Data. The literature consisted mostly of case series and small retrospective cohort studies, spanning 1988–2021. Magnet field strength was reported in 36 (63.2%) studies, with most using standard-field-strength MR imaging (1T–3T), whereas 1 study used 7T imaging. MR imaging sequences were reported in 43 (75.4%) studies. The most used sequences included T1-weighted SE (100%, 43/43), T2-weighted SE (55.8%, 24/43), dynamic postcontrast studies (48.8%, 21/43), and SPGR (44.2%, 19/43). In all studies, the diagnosis of CD was established by either surgical findings or, in the absence of histology, biochemical remission after surgery.

### Overall Sensitivity

In patients with CD, MR imaging had an overall sensitivity of 73.4% (95% CI, 68.8%–77.7%) and there was significant heterogeneity between studies ( $I^2 = 92.1\%$ ) (Online Supplemental Data). In studies that included only microadenomas, the overall sensitivity was 71.8% (95% CI, 63.0%–79.2%) and there was significant heterogeneity between studies ( $I^2 = 82.0\%$ ). In studies that included both macroadenomas and microadenomas, the sensitivity for detecting microadenomas was similar (70.0%; 95% CI, 64.9%–74.7%;  $I^2 = 91.7\%$ ) to that in studies of exclusively microadenomas ( $P = .85$ ). Combined, the sensitivity of MR imaging for all microadenomas was 70.6% (95% CI, 66.2%–74.6%;  $I^2 = 89.7\%$ ). Compared with all patients with CD, the sensitivity of MR imaging for detecting microadenomas was significantly lower when assessing either studies of exclusively microadenomas (OR = 1.18,  $P = .03$ ) or microadenomas within all studies (OR = 1.22,  $P < .001$ ).

### Study Year

Studies were categorized by year of publication into 1 of 3 epochs: pre-2000; 2000–2010; or post-2010. When the sensitivity of MR imaging was provided for different epochs within a study, data were separated into the relevant era. The sensitivity of MR imaging in the pre-2000 epoch was similar to that in the 2000–2010 epoch (60.5% versus 57.8%,  $P = .89$ ). The post-2010 era had greater sensitivity than the pre-2000 (80.1% versus 60.5%,  $P < .001$ ) and the 2000–2010 (80.1% versus 57.8%,  $P < .001$ ) eras.

### Patient Age

Two studies exclusively analyzed pediatric patients, while 12 studies exclusively analyzed adults. One additional study stratified results by patient age, and the data were included in the relevant

age group. MR imaging had greater sensitivity in adults with CD than in children (70.9% versus 52.5%,  $P < .001$ ).

### Field Strength

Twenty studies were performed using a single magnet field strength, while an additional 5 studies stratified results by field strength. Overall, there was a trend toward increasing sensitivity with increasing field strength. Compared with a standard field strength of 1.5T, scans performed at 3T identified significantly more adenomas (81.7% versus 73.6%, OR = 1.60,  $P = .03$ ).

Comparisons with low-strength (eg, 0.5T) and higher-strength (eg, 7T) magnets were limited by the small sample size. Three studies assessed the same cohort of patients on 1.5T and 3T scanners,<sup>30–32</sup> for a total of 28 patients. 3T field strength tended to be more sensitive (60.7% versus 35.7%,  $P = .10$ ). The single study comparing 1.5T and 7T images also tended toward greater sensitivity with higher field strengths (81.3% versus 43.8%,  $P = .07$ ).<sup>33</sup>

### Section Thickness

Thirty-two studies reported MR imaging sequence details, including minimum section thickness. Section thickness was categorized into 3 groups:  $>2$ ,  $\leq 1$ , and 1.1–2 mm. Compared with MR imaging protocols in which the thinnest cuts were  $>2$  mm, those with slices of 1.1–2 mm (65.6% versus 58.1%,  $P = .01$ ) and  $\leq 1$  mm (83.7% versus 58.1%,  $P < .001$ ) were significantly more sensitive.

Because studies of  $<1$  mm were more likely to have dynamic imaging, a separate analysis was performed excluding studies with dynamic contrast-enhanced sequences. Fine-section ( $\leq 1$  mm) imaging improved the sensitivity of MR imaging even in the absence of dynamic sequences compared with either 1.1- to 2-mm slices ( $P = .02$ ) or  $>2$ -mm slices ( $P = .03$ ).

### MR Imaging Sequences

Thirty-nine studies reported sensitivity for specific MR imaging sequences. Compared with noncontrast T1 SE sequences, routine postgadolinium T1 SE sequences trended toward greater sensitivity but did not reach statistical significance. However, dynamic image acquisition improved the sensitivity of gadolinium-enhanced T1-weighted SE sequences significantly (78.6% versus 58.8%,  $P < .001$ ). The sensitivity of dynamic sequences improved between the 2000 and 2010 era and the post-2010 era (52.8% versus 81.4%,  $P < .001$ ). Spoiled gradient-echo sequences (most commonly SPGR) also demonstrated increased sensitivity compared with postcontrast T1-weighted SE images (69.8% versus 58.8%,  $P < .001$ ). 3D FSE sequences (eg, SPACE) similarly demonstrated greater sensitivity than postcontrast 2D T1-weighted SE studies (82.1% versus 58.8%,  $P < .001$ ).

Given that the sensitivity of each sequence is dependent on many factors including the characteristics of the population being tested, section thickness, and magnet strength (see above), a separate analysis was performed that included only studies with direct comparisons of MR images obtained on the same population on the same scanners.

Similar to the initial analysis, there was no significant difference between noncontrast and postcontrast 2D T1-weighted SE sequences (46.8% versus 62.2%,  $P = .19$ ). Again, dynamic image acquisition improved the sensitivity of gadolinium-enhanced 2D

## Effect of MR imaging detection on surgical outcome

|               | Remission | Persistent | %    | P Value | OR (95% CI)      |
|---------------|-----------|------------|------|---------|------------------|
| All adenomas  |           |            |      |         |                  |
| MR imaging+   | 1968      | 445        | 81.6 | <.001   | 1.40 (1.16–1.68) |
| MR imaging–   | 710       | 224        | 76.0 | REF     | REF              |
| Microadenomas |           |            |      |         |                  |
| MR imaging+   | 1129      | 203        | 84.8 | <.001   | 2.63 (2.06–3.35) |
| MR imaging–   | 324       | 153        | 67.9 | REF     | REF              |

Note:—REF indicates reference value; +, detected; –, not detected.

T1-weighted SE sequences (64.8% versus 47.3%,  $P = .006$ ). There was no difference between SPGR and dynamic sequences (60.1% versus 67.3%,  $P = .21$ ); however, SPGR demonstrated improved sensitivity in comparison with postcontrast 2D T1-weighted SE sequences (55.3% versus 38.6%,  $P < .001$ ). Single studies demonstrated greater sensitivity of postcontrast 3D fast FSE sequences (eg, T2-SPACE) compared with dynamic acquisitions ( $P = .01$ )<sup>34</sup> and postcontrast 2D T1-weighted SE sequences ( $P < .001$ ).<sup>35</sup> The addition of FLAIR sequences to SPGR increased the sensitivity of MR imaging, though overall numbers were small.<sup>23</sup> T2-CISS sequences in isolation were similarly as sensitive as postcontrast 2D T1-weighted SE sequences; however, both sequences identified particular adenomas that the other did not, suggesting these sequences are complementary.<sup>36</sup>

## Significance of MR Imaging Localization for Postoperative Remission

Postoperative biochemical remission data were available in 23 studies. Overall, patients with adenomas identifiable on MR imaging had a greater rate of postoperative biochemical remission (81.6% versus 76.0%,  $P < .001$ ) (Table). Given that macroadenomas are more likely to be invasive and some may be giant and not amenable to gross total resection, a separate analysis was performed in microadenoma studies. Data pertaining only to microadenomas could be extracted from 16 studies. The strong predictive effect of MR imaging visibility on remission rates was maintained (84.8% versus 67.9%,  $P < .001$ ). There was no difference in remission rates in MR imaging–negative disease between epochs.

## DISCUSSION

### Key Results

MR imaging identifies 73% of all adenomas and 71% of microadenomas in patients with CD. Sensitivity has improved with time due to greater spatial resolution (including finer section thickness) and scanning at higher field strengths, which allows high-resolution imaging with greater SNR. The increase in detection rates may, however, come at the cost of increased false-positives. Dynamic imaging and advanced 3D MR imaging techniques (SPGR, SPACE) may improve the sensitivity over conventional 2D SE sequences alone; however, they are likely complementary rather than interchangeable. MR imaging detection is a strong predictor of remission.

### Generalizability

Perhaps the most important factor determining the sensitivity of MR imaging is how the images are interpreted. Experienced

radiologists and pituitary surgeons do not have perfect agreement among themselves<sup>33,37</sup> or each other.<sup>38</sup> Dynamic<sup>37</sup> and higher-field-strength studies<sup>33</sup> tend to demonstrate less agreement, likely due poorer specificity related to artifacts and the more heterogeneous appearance of the gland at higher resolution. The MR pulse sequences and high-field-strength (7T) imaging described in this review may not be available in all centers.

### Limitations

Significant ( $I^2 = 90\%$ ) heterogeneity between studies limits the strength of our conclusions. The sensitivity of MR imaging is determined by many factors outside the acquisition, such as image interpretation and tumor characteristics, which will differ among cohorts. The factors analyzed in the study are inherently interrelated, with higher-field-strength scanners, advanced sequences, and thinner-section acquisitions more common in later decades. Improvements in scanner technology extend beyond field strength. With time, matrix size (ie, in-plane resolution) has increased, as has the number and design of head coils (ie, channels), resulting in higher-resolution imaging with improved signal. These specifications were rarely reported; comparison by field strength alone may oversimplify interscanner differences. Although increasing spatial resolution and advanced sequences may improve sensitivity, the effect on specificity has not been consistently reported. The false-positive rate may exceed 20% in some series,<sup>39</sup> and clinicians should be cognizant of the potential for a greater rate of false-positive results with fine-section acquisitions, higher-field-strength magnets, and more advanced pulse sequences.<sup>38</sup>

### The Future

Perfectly sensitive sellar imaging would facilitate a totally noninvasive work-up of CD and high rates of surgical cure. Steps toward this goal have already been taken; however, there remains room for improvement. CD-specific MR imaging protocols have been proposed,<sup>40,41</sup> using dynamic imaging, SPGR, and volumetric FSE sequences, which are supported by our data. The benefits of higher-field-strength magnets are promising but may be limited by amplified artifacts from skull base pneumatization and bone-soft tissue interfaces. Nevertheless, the single study that compared 1.5T and 7T acquisitions demonstrated almost twice the sensitivity with higher-field-strength imaging. Gadolinium dose is a further variable to be optimized,<sup>42</sup> with half-dose acquisitions demonstrating improved sensitivity. These advances are promising but need to be weighed against the potential increased rate of false-positive results. Future studies should universally report false-positive findings.

Intraoperative MR imaging is increasingly recognized as a valuable adjunct to increase the extent of resection of macroadenomas in specialist centers,<sup>43</sup> especially as field strength improves.<sup>44</sup> The role of intraoperative MR imaging in microadenoma surgery has not been established but may be limited by air and blood artifacts



from the operation. Endosphenoidal coils may dramatically augment SNR but are currently experimental.<sup>45</sup>

Current MR imaging protocols appear particularly insensitive for detecting dural invasion, which has prognostic significance.<sup>46</sup> Preoperative detection would facilitate consideration of resection of the medial wall of the cavernous sinus, theoretically increasing the chance of cure.<sup>47</sup>

PET using [<sup>18</sup>F] fluoroethyl-L-tyrosine and <sup>11</sup>C-methionine may localize MR imaging-occult lesions.<sup>48</sup> Response to corticotropin-releasing hormone (CRH) stimulation can predict PET-positive adenomas,<sup>49</sup> and PET detection can be further improved by CRH stimulation.<sup>50</sup> Although PET may be less sensitive than advanced MR imaging sequences in isolation,<sup>49</sup> it can help confirm equivocal MR imaging findings and may be fused to volumetric MR imaging acquisitions for intraoperative stereotaxis. Recently, <sup>68</sup>Ga-tagged CRH has been demonstrated to localize CD adenomas with impressive accuracy;<sup>51</sup> however, its role in adenomas that fail to respond to CRH stimulation (approximately 10%) is unclear.

## CONCLUSIONS

MR imaging detects between two-thirds and three-quarters of adenomas causing CD. MR imaging localization significantly improves outcome in patients with CD; in microadenomas, it increases the chance of remission by almost 20%. We have illustrated the patient and imaging factors that influence detection rates. These findings will help guide improvements in MR imaging protocols to maximize the chance of cure, thus improving quality of life and longevity for patients with CD. More precision in MR imaging protocols is required in this era of precision medicine.

## ACKNOWLEDGMENT

The first author (M.C.-K.) is undertaking a higher degree funded by an Australian Government Research Training Program Scholarship.

Disclosure forms provided by the authors are available with the full text and PDF of this article at [www.ajnr.org](http://www.ajnr.org).

## REFERENCES

- Castle-Kirsbaum M, Wang YY, King J, et al. **Quality of life following endoscopic surgical management of pituitary adenomas.** *Neurosurgery* 2022;90:81–91 [CrossRef Medline](#)
- Ntali G, Asimakopoulou A, Siamatras T, et al. **Mortality in Cushing's syndrome: systematic analysis of a large series with prolonged follow-up.** *Eur J Endocrinol* 2013;169:715–23 [CrossRef Medline](#)
- Chowdhury IN, Sinaii N, Oldfield EH, et al. **A change in pituitary magnetic resonance imaging protocol detects ACTH-secreting tumours in patients with previously negative results.** *Clin Endocrinol (Oxf)* 2010;72:502–06 [CrossRef Medline](#)
- Batista D, Courkoutsakis NA, Oldfield EH, et al. **Detection of adrenocorticotropin-secreting pituitary adenomas by magnetic resonance imaging in children and adolescents with Cushing disease.** *J Clin Endocrinol Metab* 2005;90:5134–40 [CrossRef Medline](#)
- Patronas N, Bulakbasi N, Stratakis CA, et al. **Spoiled gradient recalled acquisition in the steady state technique is superior to conventional postcontrast spin echo technique for magnetic resonance imaging detection of adrenocorticotropin-secreting pituitary tumors.** *J Clin Endocrinol Metab* 2003;88:1565–69 [CrossRef Medline](#)
- Jagannathan J, Smith R, DeVroom HL, et al. **Outcome of using the histological pseudocapsule as a surgical capsule in Cushing disease: clinical article.** *J Neurosurg* 2009;111:531–39 [CrossRef Medline](#)
- Lonser RR, Wind JJ, Nieman LK, et al. **Outcome of surgical treatment of 200 children with Cushing's disease.** *J Clin Endocrinol Metab* 2013;98:892–901 [CrossRef Medline](#)
- Cristante J, Lefournier V, Sturm N, et al. **Why we should still treat by neurosurgery patients with Cushing disease and a normal or inconclusive pituitary MRI.** *J Clin Endocrinol Metab* 2019 May 14 [Epub ahead of print] [CrossRef Medline](#)
- Dai C, Feng M, Sun B, et al. **Surgical outcome of transsphenoidal surgery in Cushing's disease: a case series of 1106 patients from a single center over 30 years.** *Endocrine* 2022;75:219–27 [CrossRef Medline](#)
- Lonser RR, Nieman L, Oldfield EH. **Cushing's disease: pathobiology, diagnosis, and management.** *J Neurosurg* 2017;126:404–17 [CrossRef Medline](#)
- Wind JJ, Lonser RR, Nieman LK, et al. **The lateralization accuracy of inferior petrosal sinus sampling in 501 patients with Cushing's disease.** *J Clin Endocrinol Metab* 2013;98:2285–93 [CrossRef Medline](#)
- Feng M, Liu Z, Liu X, et al. **Diagnosis and outcomes of 341 patients with Cushing's disease following transsphenoid surgery: a single-center experience.** *World Neurosurg* 2018;109:e75–80 [CrossRef Medline](#)
- Rhoton AL. **The sellar region.** *Neurosurgery* 2002;51:S335–74 [Medline](#)
- Castle-Kirsbaum M, Uren B, Goldschlager T. **Anatomical variation for the endoscopic endonasal transsphenoidal approach.** *World Neurosurg* 2021;156:111–19 [CrossRef Medline](#)
- Parkinson D. **Extradural neural axis compartment.** *J Neurosurg* 2000;92:585–88 [CrossRef Medline](#)
- Bonneville JF, Bonneville F, Cattin F, et al. *MRI of the Pituitary Gland.* Springer-Verlag International Publishing; 2016
- Castle-Kirsbaum M, Maingard J, Lim RP, et al. **Four-dimensional magnetic resonance imaging assessment of intracranial aneurysms: a state-of-the-art review.** *Neurosurgery* 2020;87:453–65 [CrossRef Medline](#)
- Manavela MP, Goodall CM, Katz SB, et al. **The association of Cushing's disease and primary empty sella turcica.** *Pituitary* 2001;4:145–51 [CrossRef Medline](#)
- Himes BT, Bhargava AG, Brown DA, et al. **Does pituitary compression/empty sella syndrome contribute to MRI-negative Cushing's disease? A single-institution experience.** *Neurosurg Focus* 2020;48:E3 [CrossRef Medline](#)
- Miki Y, Matsuo M, Nishizawa S, et al. **Pituitary adenomas and normal pituitary tissue: enhancement patterns on gadopentetate-enhanced MR imaging.** *Radiology* 1990;177:35–38 [CrossRef Medline](#)
- Viacava P, Gasperi M, Acerbi G, et al. **Microvascular density and vascular endothelial growth factor expression in normal pituitary tissue and pituitary adenomas.** *J Endocrinol Invest* 2003;26:23–28 [CrossRef Medline](#)
- Perez-Millan MI, Berner SI, Luque GM, et al. **Enhanced nestin expression and small blood vessels in human pituitary adenomas.** *Pituitary* 2013;16:303–10 [CrossRef Medline](#)
- Chatain GP, Patronas N, Smirniotopoulos JG, et al. **Potential utility of FLAIR in MRI-negative Cushing's disease.** *J Neurosurg* 2018;129:620–28 [CrossRef Medline](#)
- Pui MH, Fok EC. **MR imaging of the brain: comparison of gradient-echo and spin-echo pulse sequences.** *AJR Am J Roentgenol* 1995;165:959–62 [CrossRef Medline](#)
- Wang J, Wu Y, Yao Z, et al. **Assessment of pituitary micro-lesions using 3D sampling perfection with application-optimized contrasts using different flip-angle evolutions.** *Neuroradiology* 2014;56:1047–53 [CrossRef Medline](#)
- Baumert B, Wörtler K, Steffinger D, et al. **Assessment of the internal craniocervical ligaments with a new magnetic resonance imaging sequence: three-dimensional turbo spin echo with variable flip-angle distribution (SPACE).** *Magn Reson Imaging* 2009;27:954–60 [CrossRef Medline](#)
- Watanabe Y, Makidono A, Nakamura M, et al. **3D MR cisternography to identify distal dural rings: comparison of 3D-CISS and 3D-SPACE sequences.** *Magn Reson Med Sci* 2011;10:29–32 [CrossRef Medline](#)

28. Moher D, Liberati A, Tetzlaff J, et al; for the PRISMA Group. Preferred reporting items for systematic reviews and meta-analyses: the PRISMA statement. *BMJ* 2009;339:b2535–53 [CrossRef Medline](#)
29. Slim K, Nini E, Forestier D, et al. Methodological index for non-randomized studies (MINORS): development and validation of a new instrument. *ANZ J Surg* 2003;73:712–16 [CrossRef Medline](#)
30. Erickson D, Erickson B, Watson R, et al. 3 Tesla magnetic resonance imaging with and without corticotropin releasing hormone stimulation for the detection of microadenomas in Cushing's syndrome. *Clin Endocrinol (Oxf)* 2010;72:793–99 [CrossRef Medline](#)
31. Kim LJ, Lekovic GP, White WL, et al. Preliminary experience with 3-Tesla MRI and Cushing's disease. *Skull Base* 2007;17:273–77 [CrossRef Medline](#)
32. Stobo DB, Lindsay RS, Connell JM, et al. Initial experience of 3 Tesla versus conventional field strength magnetic resonance imaging of small functioning pituitary tumours. *Clin Endocrinol (Oxf)* 2011;75:673–77 [CrossRef Medline](#)
33. de Rotte AA, Groenewegen A, Rutgers DR, et al. High-resolution pituitary gland MRI at 7.0 Tesla: a clinical evaluation in Cushing's disease. *Eur Radiol* 2016;26:271–77 [CrossRef Medline](#)
34. Wu Y, Cai Y, Rui W, et al. Contrast-enhanced 3D-T2-weighted SPACE sequence for MRI detection and localization of adrenocorticotropin (ACTH)-secreting pituitary microadenomas. *Clin Endocrinol (Oxf)* 2022;96:578–88 [CrossRef Medline](#)
35. Zhang K, Shen M, Qiao N, et al. Surgical outcomes and multidisciplinary management strategy of Cushing's disease: a single-center experience in China. *Neurosurg Focus* 2020;48:E7 [CrossRef Medline](#)
36. Lang M, Habboub G, Moon D, et al. Comparison of constructive interference in steady-state and T1-weighted MRI sequence at detecting pituitary adenomas in Cushing's disease patients. *J Neurol Surg B Skull Base* 2018;79:593–98 [CrossRef Medline](#)
37. Tabarin A, Laurent F, Catargi B, et al. Comparative evaluation of conventional and dynamic magnetic resonance imaging of the pituitary gland for the diagnosis of Cushing's disease. *Clin Endocrinol (Oxf)* 1998;49:293–300 [CrossRef Medline](#)
38. Grober Y, Grober H, Wintermark M, et al. Comparison of MRI techniques for detecting microadenomas in Cushing's disease. *J Neurosurg* 2018;128:1051–57 [CrossRef Medline](#)
39. Yogi-Morren D, Habra MA, Faiman C, et al. Pituitary MRI findings in patients with pituitary and ectopic ACTH-dependent Cushing syndrome: does a 6-mm pituitary tumor size cut-off value exclude ectopic ACTH syndrome? *Endocr Pract* 2015;21:1098–103 [CrossRef Medline](#)
40. Vitale G, Tortora F, Baldelli R; A.B.C. Group, et al. Pituitary magnetic resonance imaging in Cushing's disease. *Endocrine* 2017;55:691–99 [CrossRef Medline](#)
41. Bashari WA, Gillett D, MacFarlane J, et al. Modern imaging in Cushing's disease. *Pituitary* 2022;25:709–12 [CrossRef Medline](#)
42. Portocarrero-Ortiz L, Bonifacio-Delgadillo D, Sotomayor-González A, et al. A modified protocol using half-dose gadolinium in dynamic 3-Tesla magnetic resonance imaging for detection of ACTH-secreting pituitary tumors. *Pituitary* 2010;13:230–35 [CrossRef Medline](#)
43. Coburger J, König R, Seitz K, et al. Determining the utility of intraoperative magnetic resonance imaging for transsphenoidal surgery: a retrospective study: clinical article. *J Neurosurg* 2014;120:346–56 [CrossRef Medline](#)
44. Jones PS, Swearingen B. Intraoperative MRI for pituitary adenomas. *Neurosurg Clin N Am* 2019;30:413–20 [CrossRef Medline](#)
45. Chittiboina P, Talagala SL, Merkle H, et al. Endosphenoidal coil for intraoperative magnetic resonance imaging of the pituitary gland during transsphenoidal surgery. *J Neurosurg* 2016;125:1451–59 [CrossRef Medline](#)
46. Lonser RR, Ksendzovsky A, Wind JJ, et al. Prospective evaluation of the characteristics and incidence of adenoma-associated dural invasion in Cushing disease. *J Neurosurg* 2012;116:272–79 [CrossRef Medline](#)
47. Cohen-Cohen S, Gardner PA, Alves-Belo JT, et al. The medial wall of the cavernous sinus, Part 2: selective medial wall resection in 50 pituitary adenoma patients. *J Neurosurg* 2018;131:131–40 [CrossRef Medline](#)
48. Berkmann S, Roethlisberger M, Mueller B, et al. Selective resection of Cushing microadenoma guided by preoperative hybrid 18-fluoroethyl-L-tyrosine and 11-C-methionine PET/MRI. *Pituitary* 2021;24:878–86 [CrossRef Medline](#)
49. Chittiboina P, Montgomery BK, Millo C, et al. High-resolution (18)F-fluorodeoxyglucose positron emission tomography and magnetic resonance imaging for pituitary adenoma detection in Cushing disease. *J Neurosurg* 2015;122:791–97 [CrossRef Medline](#)
50. Boyle J, Patronas NJ, Smirniotopoulos J, et al. CRH stimulation improves (18)F-FDG-PET detection of pituitary adenomas in Cushing's disease. *Endocrine* 2019;65:155–65 [CrossRef Medline](#)
51. Walia R, Gupta R, Bhansali A, et al. Molecular imaging targeting corticotropin-releasing hormone receptor for corticotropinoma: a changing paradigm. *J Clin Endocrinol Metab* 2021;106:e1816–26 [CrossRef Medline](#)